

Excitation of isoscalar giant resonances and monopole giant resonance splitting in actinide nuclei

H. P. Morsch, M. Rogge, P. Turek, C. Mayer-Böricke, and P. Decowski
Institut für Kernphysik, Kernforschungsanlage Jülich, D-5170 Jülich, West Germany
 (Received 28 October 1981)

Scattering of 100 and 172 MeV α particles has been used to study giant resonances in ^{232}Th and ^{238}U . First, experiments have been performed at scattering angles between 8 and 17° using a 1 m scattering chamber. Consistent fits to these data at both incident energies indicate that the giant monopole resonance in these nuclei splits into two parts separated by more than 4 MeV. This is confirmed by new magnetic spectrograph results which have been obtained in the angular region 3°–5°. A splitting of the monopole strength as deduced from our data can be explained by mixing of giant monopole and quadrupole resonances in these deformed nuclei. From the angular dependence of the differential cross sections evidence for the existence of odd parity ($L=1,3$) giant resonances at high excitation energies is obtained. From the small angle data the giant octupole resonance was located at $E_x = 19.6 \pm 1$ MeV with a width $\Gamma(\text{FWHM}) = 6.5 \pm 1$ MeV.

[NUCLEAR REACTIONS $^{232}\text{Th}, ^{238}\text{U}(\alpha, \alpha')$; $E_\alpha = 100$ and 172 MeV;
 measured $\sigma(\Theta)$. Deduced excitation strengths for multipolarities
 $L=0-4$, splitting of the $L=0$ strength.]

I. INTRODUCTION

During the last few years strong efforts have been made¹⁻³ to study the giant monopole resonance (GMR). In heavy nuclei a concentrated GMR is observed at $E_x \sim 80 A^{-1/3}$ MeV which exhausts approximately the full energy weighted sum rule (EWSR) strength. In a more detailed discussion, the question arises whether in the region of deformed nuclei the GMR is affected by deformation. On the basis of the liquid drop model deformation effects are not expected. However, in a more refined picture the GMR can mix with the giant quadrupole resonance (GQR) leading to a splitting of the monopole strength.^{4,5} Experimental evidence for deformation effects in the monopole excitation has been reported^{6,7} mainly for rare earth nuclei: a shift to slightly higher excitation energies and a sum rule strength smaller than found for neighboring spherical nuclei. However, no clear evidence for the existence of a low energy monopole component has yet been obtained.

To study the GMR in deformed actinide nuclei we investigated α scattering at different incident energies. Based on the results of Ref. 2, we expect at 100 MeV incident energy a rather weak excitation of the GMR, so dominantly the GQR should be observed. At 172 MeV we expect both, GQR and GMR, to be strongly excited. Thus, from a careful comparison of low and high energy data the GMR

excitation may be deduced. For Pb this method yielded results² in good agreement with small angle studies.^{1,3} Another motivation for our experiment was a more systematic study of the new odd parity giant resonances found in ^{208}Pb at higher excitation energies (Refs. 8 and 9).

II. EXPERIMENTS AND DATA ANALYSIS

The experiments were performed using momentum analyzed α beams of 100 and 172 MeV from the Jülich isochronous cyclotron JULIC. Experiments were performed at scattering angles between 8° and 17° using a 1 m scattering chamber. In addition, small angle scattering data are discussed which have been measured with the new Jülich magnetic spectrograph BIG KARL.

A. Larger angle measurements

The details of the experimental setup were the same as in Refs. 2, 8, and 10. Self-supporting ^{232}Th and ^{238}U targets of about 8 mg/cm² thickness were used. Although considerable care was taken in preparing the targets contamination of H, C, and O could not be avoided. Therefore, separate contaminant spectra were measured (Fig. 1). Great care was taken to subtract the contaminant peaks in the

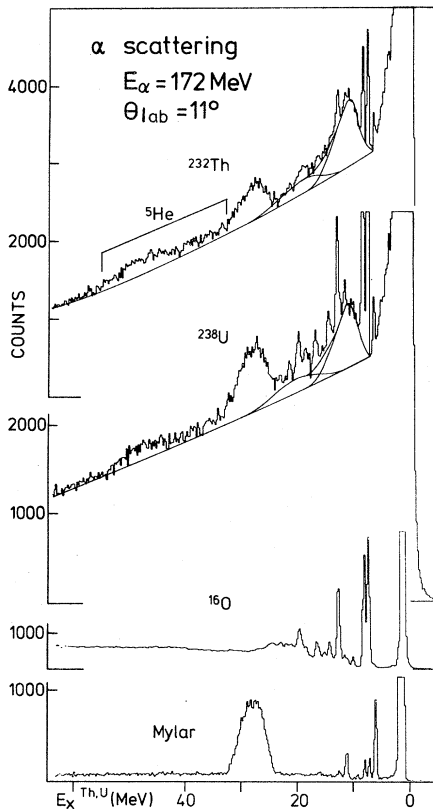


FIG. 1. Spectra of 172 MeV α scattering from ^{232}Th , ^{238}U in comparison with contaminant spectra from ^{16}O and Mylar (C-H). Background and fits to the giant resonance region are indicated as well as the decomposition into even ($L=0,2$) and odd parity ($L=1,3$) giant resonance bumps at $E_x \sim 11$ and 20 MeV, respectively.

Th and U spectra. As a check, for several angles complete contaminant spectra have been subtracted (see the 172 MeV spectra in Fig. 2). In the spectra shown in Figs. 1 and 2 the background assumed was of simple form similar to that in Ref. 8: The high energy part of the spectra above 30 MeV was extended to the minimum of the low energy part of the spectra at 7 MeV by a smooth polynomial fit. It was made sure that the angular dependence of the background (shown in Fig. 3 for the GQR) was smooth. Taking into account the contaminations and the background two bumps remain in the spectra. They are indicated by solid lines in Fig. 1. The larger one at about 11 MeV excitation energy shows an angular distribution typical for even parity excitations ($L=0, 2$, and 4), whereas the smaller one at about 20 MeV has an angular distribution which is out of phase with the first one indicating odd parity excitations ($L=1,3$) (Refs. 8 and 9).

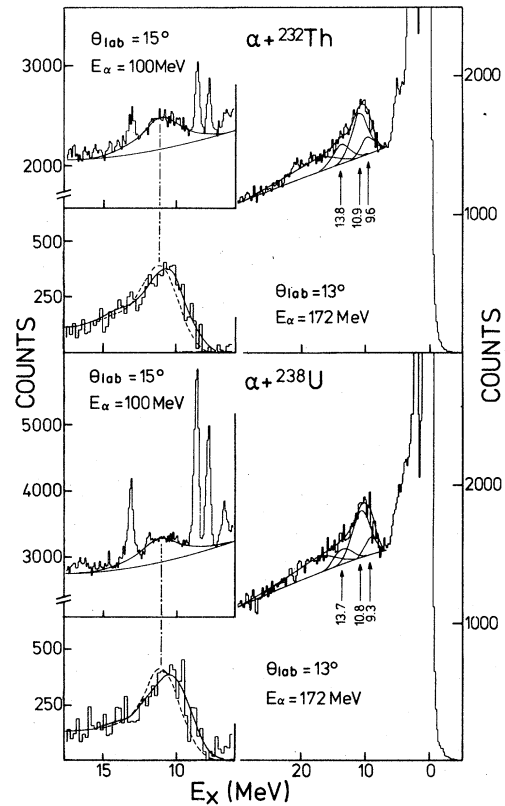


FIG. 2. Spectra of 100 and 172 MeV α scattering from ^{232}Th and ^{238}U . Background and fits to the giant resonance region are indicated as well as the decomposition into separate peaks for the resonances indicated by arrows and a high lying bump at $E_x \sim 20$ MeV. Left bottom parts: giant resonance data (from the right hand spectra) after background subtraction.

The disentangling of excitations of the same parity is more difficult. For the even parity excitations this was done by measuring at different incident energies. For the lower incident energy raw spectra are shown in the inset of Fig. 2. Several 100 MeV spectra have been taken between scattering angles of 11° and 15° . They show a quite symmetric giant resonance peak which is mainly due to $L=2$ excitation.¹¹ Quite different, at 172 MeV an asymmetric shape of the giant resonance bump is observed (Fig. 2). (As will be shown later, this is due to a much stronger excitation of the GMR and the excitation of the new giant resonances⁸ at $E_x \sim 20$ MeV.) In addition, the giant resonance maximum is shifted in the 172 MeV data to lower excitation energies (by about 0.6 MeV) in comparison with the position of the peak in the 100 MeV spectra (see the lower left hand spectra in Fig. 2). Both the 100 and 172 MeV

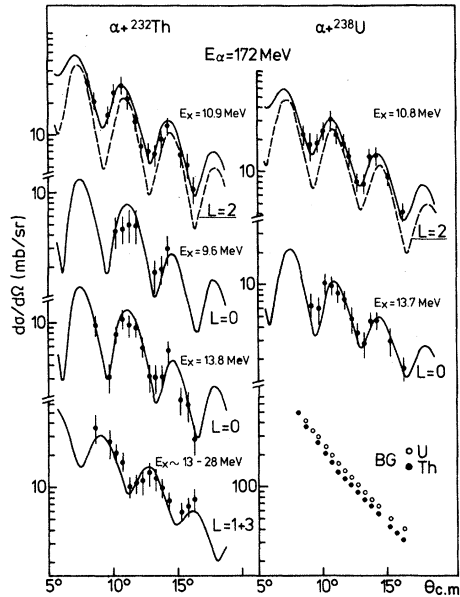


FIG. 3. Differential cross sections in comparison with microscopic DWBA calculations. The angular dependence of the background in the region of the GQR is shown in the right bottom part.

spectra were taken in the same experimental run ensuring that the relative energy calibration for the different energies is known with sufficiently high accuracy (< 100 keV).

In a first attempt to fit the data four Gaussian peaks (as in Ref. 8) were assumed representing GQR, GMR, and (only for the 172 MeV fits) two higher energy resonances. A fit with one Gaussian peak for GQR and GMR as used at $E_\alpha = 120$ MeV (Ref. 11) is not possible at the higher incident energy because of larger $L=0$ cross sections.² The higher energy broad structure ($E_x \sim 20$ MeV) can be

fitted almost equally well by one Gaussian peak at most angles. However, the use of two peaks yields better fits for all angles; further, it does not add uncertainties in the total yield which is discussed only. The position of the GQR (which may have some contributions of higher L) is mainly fixed by the 100 MeV data, whereas the GMR parameters were fixed by the analysis for both incident energies. The 100 MeV fits were quite similar to those shown in Fig. 2. However, for 172 MeV fits were obtained which are given by the dashed lines. These fits peak at the position of the experimental giant resonance bump in the 100 MeV spectra (as indicated by the dotted-dashed line in Fig. 2) and do not reproduce the 0.6 MeV shift mentioned above. This result is in contrast to the case of ^{208}Pb for which a consistent fit of low and high energy data was achieved² (in the Pb data there was no shift of giant resonance maxima at different beam energies).

In order to get better fits an additional resonance peak had to be assumed in the low excitation region of the GQR. The results are shown in Fig. 2 by the solid fit lines in the lower left hand parts (background subtracted 172 MeV data) and in the 172 MeV spectra on the right hand side. They represent the minimum number of peaks required to obtain a good fit at both beam energies: Taking into account the 172 MeV data only, the positive parity excitations could be fitted by two peaks whereas the 100 MeV data alone can be fitted by one. However, in such an analysis the peak positions at different beam energies do not match. Therefore, a consistent fit to all data requires the assumption of three peaks. The resonance parameters are given in Table I except for the high lying resonances which were assumed at $E_x = 17$ and 21 MeV with full width at half maximum $\Gamma(\text{FWHM}) = 5.6$ and 6.8 MeV, respectively.

Differential cross sections obtained from the 172

TABLE I. Resonance parameters and sum rule strengths (uncertainties $\pm 20\%$) for $L=0, 2,$ and 4 excitations derived from the larger angle data. The $L=0$ strengths are obtained using a transition density similar to $\rho_{\text{TR}3}$ in Ref. 10.

	E_x (MeV)	Γ (MeV)	L	S (% EWSR)
^{232}Pb	9.6 ± 0.3	2.3 ± 0.3	0	28
	10.9 ± 0.3	3.0 ± 0.4	2,4	62,10
	13.8 ± 0.4	3.0 ± 0.5	0	66
^{238}U	9.3 ± 0.3	2.0 ± 0.3	0	30
	10.8 ± 0.3	3.0 ± 0.4	2,4	66,10
	13.7 ± 0.4	3.0 ± 0.5	0	65

MeV data are presented in Fig. 3. The uncertainties in the deduced cross sections due to background subtraction and fit ambiguities were estimated to be between ± 20 and ± 30 % (indicated as error bars in Fig. 3). Consequently, also the errors in the extracted EWSR strengths (Table I) are of the order of 20%. Cross sections for the high energy bump ($E_x \sim 13$ –28 MeV) and also for the component at $E_x \sim 9.6$ MeV are given in Fig. 3 only for Th. The data for U are quite similar but have larger errors due to ^{16}O contaminations. The high energy bump is somewhat broader than in the case of ^{208}Pb . Similar to ^{208}Pb its angular dependence indicates at least two different resonances, however, with much larger uncertainties.

To analyze our experimental data in Fig. 3, distorted wave Born approximation (DWBA) calculations were performed using folding type form factors. These calculations are of the same type as those in Refs. 8, 10, and 12 using the same effective interaction. Optical potentials were obtained by fitting our elastic scattering data. The parameters are for Th: $V=170.5$ MeV, $r_V=1.19$ fm, $a_V=0.68$ fm, $W_{(\text{vol})}=20.5$ MeV, $r_W=1.48$ fm, $a_W=0.75$ fm; and for U: $V=170.6$ MeV, $r_V=1.15$ fm, $a_V=0.68$ fm, $W_{(\text{vol})}=21.4$ MeV, $r_W=1.48$ fm, $a_W=0.73$ fm; $r_c=1.3$ fm.

The results of this DWBA analysis are shown in Fig. 3. They will be discussed in Sec. III.

B. Small angle data

In this study new small angle data (scattering angles 3° – 5°) are included which were taken with the Jülich magnetic spectrograph BIG KARL.¹³ Details of these experiments as well as results for a number of nuclei will be given elsewhere.¹⁴ Spectra are given in Fig. 4. To analyze these data a linear background is assumed which is consistent with that used in the analysis of the larger angle data (Figs. 1 and 2). In the fits to the spectra narrow contaminant peaks were included as well as giant resonances as discussed above. Without any change the parameters in Table I yielded excellent fits to the data (giant resonance peaks as indicated in Fig. 4). This supports the conclusions drawn from the larger angle data, in particular, since the giant resonances are more strongly excited relative to the background. The high energy bump is well fitted by one Gaussian located at $E_x=19.6 \pm 1$ MeV with a width of 6.5 ± 1 MeV.

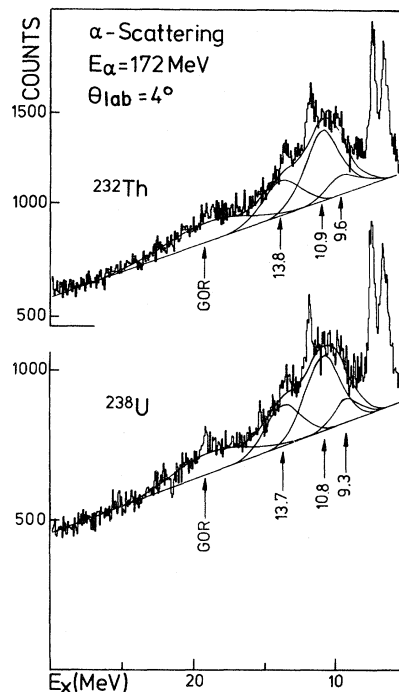


FIG. 4. Small angle spectra (4°) of 172 MeV α scattering from ^{232}Th and ^{238}U . The sharp lines in the spectra are due to ^{16}O contamination. Background and fits to giant resonances are indicated.

III. DISCUSSION

The effect of ground state deformation on the parameters of giant resonances is of considerable experimental and theoretical interest. The isovector giant dipole resonance splits into a $K=0^-$ and 1^- component with centroid energies separated by about 3 MeV in deformed actinide nuclei.¹⁵ Much smaller deformation effects are expected for the GQR which splits into three components with $K=0^+$, 1^+ , and 2^+ . Experimentally a broadening of the resonance of the order of 1 MeV has been found for rare earth nuclei.^{6,16} As the GQR in ^{208}Pb contains contributions of higher L (Ref. 10) it is interesting to study these components in deformed heavy systems. For the GMR a splitting is possible only through mixing with the $K=0^+$ component of the GQR. Also, the recently found negative parity excitations^{8,9} should show deformation effects. However, these resonances have large widths and, therefore, a study of deformation effects is more difficult. In the following we discuss structure in the GQR region, the properties of the

GMR, and the odd parity excitations at high excitation energy.

A. The giant quadrupole excitation

The angular distributions of the resonances at 10.9 and 10.8 MeV are shown in Fig. 3. They are well described by a mixture of $L=2$ and 4 excitation with strengths given in Table I. The width derived from our data is only 0.4 MeV larger than that found for the spherical nucleus ^{208}Pb ($\Gamma=2.6$ MeV, Ref. 10). This indicates a rather small deformation effect. In rare earth nuclei a larger broadening $\Delta\Gamma$ of the order of 1 MeV was found, but also with a larger width Γ of about 4 MeV (Refs. 6 and 16) in the spherical case. If the smaller deformation of the actinide nuclei ($\beta_2 \sim 0.20-0.26$, Ref. 17) is taken into account the relative broadening of the GQR is about the same in both mass regions. The GQR angular distributions in Fig. 3 show pronounced diffraction structure. This is different from ^{208}Pb for which the GQR angular distribution was quite flat.¹⁰ Although the width of the resonance is larger than in the case of ^{208}Pb , no $L=6$ (or $L=3$) component¹⁰ was needed to fit the data ($E_x \sim 10.9$ MeV) in Fig. 3. The fact that smaller contributions of larger multipolarity are found than in ^{208}Pb may indicate that due to deformation effects in the present cases the higher multipole strength is strongly spread out in energy and therefore contributes mainly to the subtracted background.

Position, width, and strength of the GQR are in good agreement with other hadron scattering re-

sults.^{11,18} Our results are not consistent with electron scattering studies.^{19,20} In (e,e') (Ref. 19) the isovector giant dipole resonance is dominant; this leads to large uncertainties in the extraction of the GQR. Also in the (e,f) work (Ref. 20) a GQR in U is obtained with too large a width of 6.9 MeV. Further it should be mentioned that the conclusions of Ref. 19 on transition densities from (e,e') are not confirmed: As for spherical nuclei, the GQR cross section (Fig. 3) is well described using a surface derivative transition density (see Ref. 10) derived from the unmodified ground state density of Ref. 21.

B. Splitting of the giant monopole resonance

The other resonances in Table I show in our analysis the expected² strong energy dependence of the $L=0$ yield which is much different from that of $L=2$ (or $L=4$). The experimental results for the resonance at ~ 13.7 MeV are in agreement with Ref. 7; the corresponding angular distributions in Fig. 3 are well described by the $L=0$ DWBA calculations. The monopole strength deduced exhausts about 65% of the EWSR limit. This is significantly smaller than found in the case of ^{208}Pb . The new structure ($E_x \sim 9.5$ MeV) has the same features as the high energy monopole resonance: Its strength is very small in the 100 MeV fits but significant contributions are obtained in the analysis of the 172 MeV data. Furthermore, its angular distribution is consistent with an $L=0$ DWBA calculation (Fig. 3). The sum rule strengths (Table I) for this resonance and the one above the GQR together exhaust

TABLE II. Sum rule strengths from the small angle data (estimated uncertainties $\pm 30\%$) in comparison with the larger angle results.

	E_x (MeV)	L	Small angle data S (% EWSR)	Larger angle data S (% EWSR)
^{232}Th	9.6	0	21	28
	10.9	2,4	63 ^a	62,10
	13.8	0	63	66
	19.6	3	42	40 ^b
^{238}U	9.3	0	22	30
	10.8	2,4	53 ^a	66,10
	13.7	0	69	65
	19.6	3	40	40 ^b

^aAssuming $L=2$ only (at these angles $L=4$ cross sections are relatively small).

^b $L=3$ yield in the excitation region 13–28 MeV.

about the same monopole sum rule strength as found for the unsplit GMR of ^{208}Pb (Ref. 10). Sum rule strengths obtained from the small angle cross sections are given in Table II assuming L assignments as deduced from the larger angle data. Generally a good agreement is obtained with the larger angle results; only the sum rule strengths for the low lying $L=0$ peaks are found to be somewhat smaller. The fact that a consistent description of small and larger angle data is obtained supports strongly our conclusions of a split monopole resonance.

A splitting of the GMR as obtained from our data is consistent with theoretical predictions.^{4,5} The low energy component of the GMR is found in the low excitation region of the GQR which should be of $K=0^+$ structure. Centroid energies and sum rule strengths of $L=0$ and 2 excitations are compared in Fig. 5 with the theoretical prediction of Ref. 5. In the calculation of Ref. 5 the sum rule strengths assumed for a spherical system were 100% both for $L=0$ and 2 excitation. This is larger than found experimentally (Ref. 10). Taking this into account then a remarkable agreement of the theoretical prediction with our experimental results is obtained.

Finally, it should be mentioned that in the description of the GMR cross sections the same difficulty exists as discussed in Ref. 10: By using the Tassie density in a folding approach a cross section

too small by a factor of 2 is obtained. In order to get a reliable sum rule strength one can either use a transition density similar to ρ_{TR3} in Ref. 10 (this was done in this study) or one may describe the GMR cross section in a potential approach.²²

C. Odd parity giant resonances at higher excitation energy

The differential cross sections for the high lying structure ($E_x \sim 13-28$ MeV) is given in Fig. 3. The angular distribution (in Fig. 3) is well described by a sum of $L=1$ and 3 excitations assuming 90% and 40% EWSR strength for $L=1$ and 3, respectively. These strengths are consistent with those for ^{208}Pb (Ref. 8). As for ^{208}Pb we would assume an $L=3$ character mainly in the lower energy region around 17 MeV whereas the $L=1, T=0$ excitation is located at the higher excitation energy. Apart from our (α, α') experiments there is a clear evidence for the high lying resonance from fission decay in the reaction $^{238}\text{U}(\alpha, \alpha'f)$. The details of this experiment will be discussed elsewhere.²³ Also in 200 MeV proton scattering an $L=1, T=0$ excitation has been found²⁴ at 21.5 MeV in ^{208}Pb with a sum rule strength consistent with our results.²⁵ However, in the experiments of Ref. 9 the high lying $L=1$ excitation has not been found.

Interestingly, in the angular range of $4^\circ-5^\circ$ covered by the small angle data the giant octupole cross sections are predicted to be large whereas $L=1$ and possible $L=5$ excitations are weak. Because of this the high lying resonance in Fig. 4 can be identified as the giant octupole resonance (GOR). The octupole yield derived from the small angle data in Table II is consistent with that deduced from the other data. In comparison with the small angle spectra there is additional yield in the larger angle spectra not only at higher excitations (expected for $L=1$) but also in the region 15–17 MeV. Consistent with random-phase approximations (RPA) calculations²⁶ this may be explained by an additional $L=5$ contribution.

IV. SUMMARY

Our study of α scattering from actinide nuclei has indicated excitation of isoscalar giant resonances with multipolarity $L=0-4(5)$. In comparison with the results for the spherical nucleus ^{208}Pb deformation effects have been found for different multipolarities. For the high lying odd parity reso-

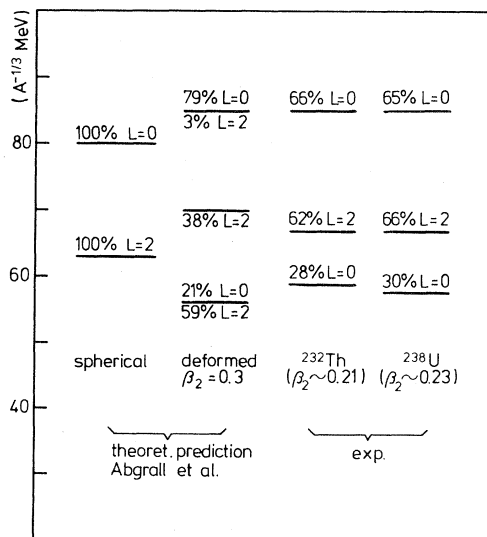


FIG. 5. Comparison of giant resonance centroid energies ($L=0$ and 2) from Table I with the theoretical prediction of Ref. 5. The deformation parameters β_2 given for Th and U are average values from Ref. 17.

nance bump—the existence of which has been confirmed for ^{232}Th and ^{288}U —there is indication for a broadening of the order of 1.5–2 MeV. However, much clearer evidence for deformation effects has been obtained for the more narrow resonances of multipolarity $L=0$ and 2. In particular, our results indicate a large splitting of the GMR; this has been predicted theoretically. Both a low and a high frequency monopole component could be located which are separated by more than 4 MeV. This represents the largest giant resonance splitting due to deformation found experimentally.

Most of the data existing on the GMR excitation have been obtained from small angle experi-

ments.^{1,3,6,7} To disentangle the low frequency monopole peak in the region of the GQR requires an accurate determination of small differences in giant resonance yields. With the “small angle” method this is possible only at extremely small angles (see the discussion in Ref. 6) where in addition to large experimental difficulties changes of the background behavior are expected.²⁷ On the other hand with our method of studying the energy dependence, small differences in the yield of $L=0$ and 2 giant resonances can be investigated at many different scattering angles. This reduces ambiguities in the extraction of resonance parameters necessary to establish the low energy monopole peak.

- ¹D. H. Youngblood, C. M. Rozsa, J. M. Moss, D. R. Brown, and J. D. Bronson, *Phys. Rev. Lett.* **39**, 1188 (1977); M. Buenerd, C. Bonhomme, D. Lebrun, P. Martin, J. Chauvin, G. Duhamel, G. Perrin, and P. de Saintignon, *Phys. Lett.* **84B**, 305 (1979).
- ²H. P. Morsch, M. Rogge, P. Turek, C. Sükösd, and C. Mayer-Böricke, *Phys. Rev. C* **20**, 1600 (1979).
- ³A. Willis, M. Morlet, N. Marty, R. Frascaria, C. Djalali, V. Comparat, and P. Kitching, *Nucl. Phys.* **A344**, 137 (1980); C. M. Rozsa, D. H. Youngblood, J. D. Bronson, Y. W. Lui, and U. Garg, *Phys. Rev. C* **21**, 1252 (1980).
- ⁴D. Zawischa, J. Speth, and D. Pal, *Nucl. Phys.* **A311**, 445 (1978).
- ⁵Y. Abgrall, B. Morand, E. Caurier, and B. Grammaticos, *Nucl. Phys.* **A346**, 431 (1980).
- ⁶U. Garg, P. Bogucki, J. D. Bronson, Y.-W. Lui, C. M. Rozsa, and D. H. Youngblood, *Phys. Rev. Lett.* **45**, 1670 (1980).
- ⁷M. Buenerd, D. Lebrun, Ph. Martin, P. de Saintignon, and C. Perrin, *Phys. Rev. Lett.* **45**, 1667 (1980).
- ⁸H. P. Morsch, M. Rogge, P. Turek, and C. Mayer-Böricke, *Phys. Rev. Lett.* **45**, 337 (1980).
- ⁹T. A. Carey, W. D. Cornelius, N. J. DiGiacomo, J. M. Moss, G. S. Adams, J. B. McClelland, G. Pauletta, C. Whitten, M. Gazzaly, N. Hintz, and C. Glashauser, *Phys. Rev. Lett.* **45**, 239 (1980); T. Yamagata, S. Kishimoto, K. Yuasa, K. Iwamoto, B. Saeki, M. Tanaka, T. Fukuda, I. Mirua, M. Inoue, and H. Ogata, *Phys. Rev. C* **23**, 937 (1981).
- ¹⁰H. P. Morsch, C. Sükösd, M. Rogge, P. Turek, H. Machner, and C. Mayer-Böricke, *Phys. Rev. C* **22**, 489 (1980).
- ¹¹M. N. Harakeh, H. P. Morsch, K. v. d. Weg, A. v. d. Woude, and F. E. Bertrand, *Phys. Rev. C* **21**, 768 (1980).
- ¹²H. P. Morsch and P. Decowski, *Phys. Lett.* **95B**, 160 (1980).
- ¹³A. Abdel Gawad, A. Hardt, S. A. Martin, J. Reich, K. L. Brown, K. Halbach, *Proceedings of the 5th International Conference on Magnet Technology, Roma, 1975*, p. 45.
- ¹⁴H. P. Morsch, P. Decowski, M. Rogge, P. Turek, L. Zemlo, S. A. Martin, G. P. A. Berg, I. Katayama, J. Meissburger, J. Römer, W. Hürlimann, J. Reich (unpublished).
- ¹⁵J. T. Caldwell, E. J. Dowdy, B. L. Berman, R. A. Alvarez, and P. Meyer, *Phys. Rev. C* **21**, 1215 (1980), and references therein.
- ¹⁶T. Kishimoto, J. M. Moss, D. H. Youngblood, J. D. Bronson, C. M. Rozsa, D. R. Brown, and A. D. Bacher, *Phys. Rev. Lett.* **35**, 552 (1975).
- ¹⁷P. David, J. Debrus, H. Essen, F. Lübke, H. Mommsen, R. Schoenmackers, W. Soyez, H. V. Geramb, and E. F. Hefter, *Z. Phys. A* **278**, 281 (1976); C. H. King, J. E. Finck, G. M. Crawley, J. A. Nolen, and R. M. Ronningen, *Phys. Rev. C* **20**, 2084 (1980).
- ¹⁸M. B. Lewis and D. J. Horen, *Phys. Rev. C* **10**, 1099 (1974).
- ¹⁹R. Pitthan, F. R. Buskirk, W. A. Houk, and R. W. Moore, *Phys. Rev. C* **21**, 28 (1980).
- ²⁰J. D. T. Arruda Neto, S. B. Herdade, B. S. Bhandari, and I. C. Nascimento *Phys. Rev. C* **18**, 863 (1978).
- ²¹C. W. Jager, H. de Vries, and C. de Vries, *Nucl. Data Tables* **14**, 479 (1974).
- ²²G. R. Satchler, *Part. Nucl.* **5**, 105 (1973); see also the detailed discussion of the GMR in F. E. Bertrand, G. R. Satchler, D. J. Horen, J. R. Wu, A. D. Bacher, G. T. Emery, W. P. Jones, D. W. Miller, and A. v. d. Woude, *Phys. Rev. C* **22**, 1832 (1980).
- ²³H. P. Morsch, M. Rogge, H. Machner, C. Sükösd, P. David, J. Debrus, H. Janszen, and J. Schulze, *Phys. Lett.* (to be published).
- ²⁴C. Djalali, N. Marty, M. Morlet, and A. Willis (unpub-

lished).

²⁵The (p,p') cross section has been calculated by using the transition density from Ref. 8 with the isoscalar dipole sum rule from P. Decowski, H. P. Morsch, and W. Benenson, Phys. Lett. 101B, 147 (1981).

²⁶R. A. Broglia, H. Esbensen, G. Pollarolo, A. Vittari, A. Winther, and C. H. Dasso, Phys. Lett. 87B, 15 (1979).

²⁷G. F. Bertsch and O. Scholten, Phys. Rev. C 25, 804 (1982).